

Electronic Supplementary Information for:

**Linking Melem with Conjugated Schiff-Base Bond to Boost
Photocatalytic Efficiency of Carbon Nitride for Overall Water
Splitting**

Hu Liu^{a,b,d†}, Mengqi Shen^{b†}, Peng Zhou^c, Zhi Guo^e, Xinyang Liu^a, Weiwei Yang^a,
Manyi Gao^a, Min Chen^f, Huanqin Guan^b, Nitin P. Padture^f, Yongsheng Yu^{a*}, Shaojun
Guo^{c*}, Shouheng Sun^{b*}

^aMIT Key Laboratory of Critical Materials Technology for New Energy Conversion and Storage, School of Chemistry and Chemical Engineering, Harbin Institute of Technology, Harbin, Heilongjiang 150001, China

^bDepartment of Chemistry, Brown University, Providence, Rhode Island 02912, USA

^cDepartment of Materials Science & Engineering, College of Engineering, Peking University, Beijing 100871, China

^dSchool of Chemistry and Chemical Engineering, Xi'an University of Architecture and Technology, Xi'an 710055, China.

^eShanghai Synchrotron Radiation Facility. Shanghai Advanced Research Institute, CAS, Shanghai 201204, China

^fSchool of Engineering, Brown University, Providence, Rhode Island 02912, USA

[†] H. Liu and M. Q. Shen contributed equally to this study.

*To whom correspondence should be addressed. Email: ysyu@hit.edu.cn, guosj@pku.edu.cn and ssun@brown.edu

1. Materials and Methods

The synthesis of the precursor monomeric unit

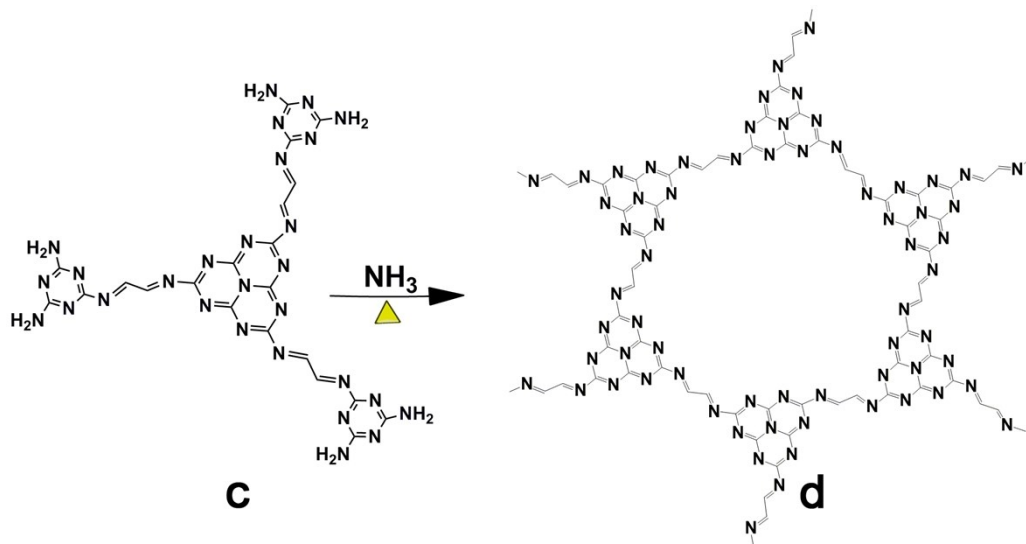
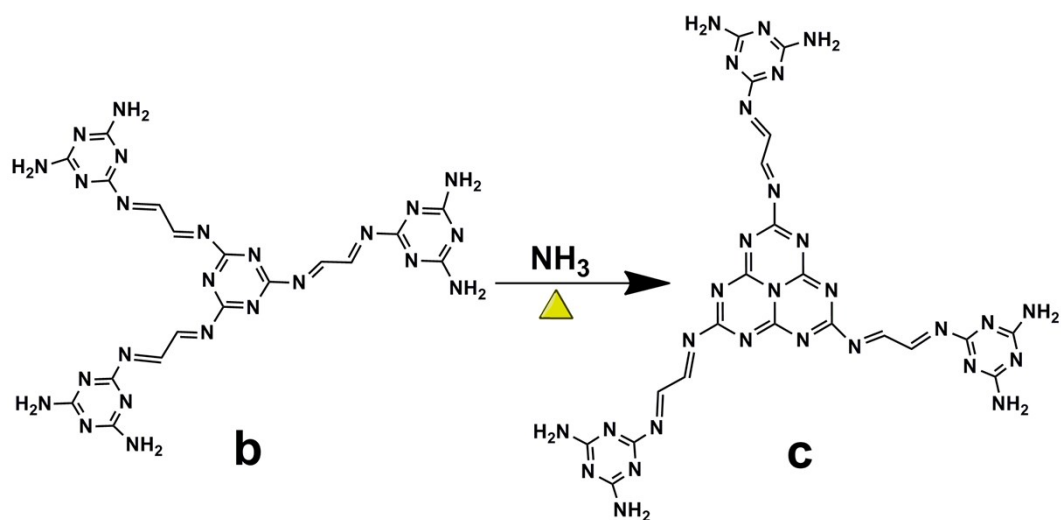
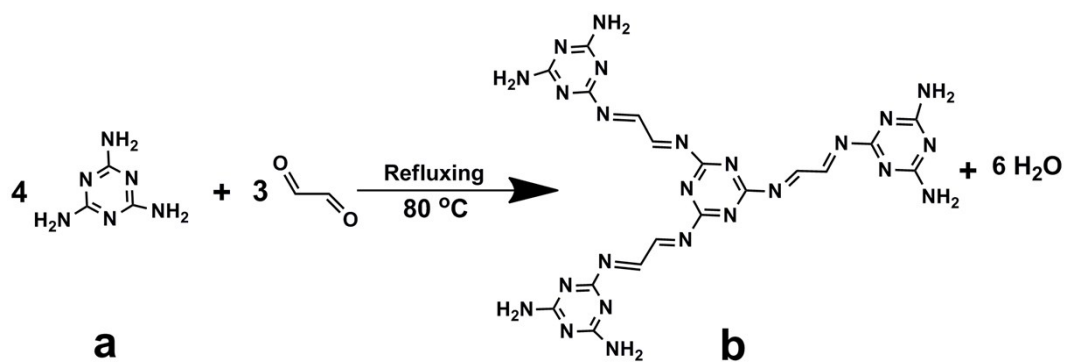
10 g melamine powder and 3 mL glyoxal aqueous solution (molar ratio of the glyoxal and melamine: 3:8) were completely dispersed into 50 mL alcohol at room temperature. Then the mixed solution was refluxed at 80 °C for 2 h and dried in 60 °C drying baker for overnight to entirely remove alcohol.

The synthesis of the $g-C_xN_4$

The synthesis of $g-C_xN_4$ undergoes three crucial steps: melem forming, triazine-carbon ring unit constructing and final thermal polymerization^[1]. For a typical synthesis process of $g-C_{3.6}N_4$, the precursor monomeric sequentially went through three stages of heating: 300 °C for 1 h, 425 °C for 1 h and 550 °C for 4 h . After naturally cooling down to room temperature, the final product was obtained for further characterization and catalytic reaction (abbreviated $g-C_{3.6}N_4$). In addition, for the other composition $g-C_xN_4$ was synthesized by the same method with controlling molar ratio of the glyoxal and melamine of 3:4, 3:16 and 0 (abbreviated $g-C_{3.8}N_4$, $g-C_{3.2}N_4$ and $g-C_3N_4$), respectively. For example, 3:4 of mole ratio of glyoxal and melamine gave $g-C_{3.8}N_4$, 3:16 of mole ratio of glyoxal and melamine designated as $g-C_{3.2}N_4$ and pure melamine yielded $g-C_3N_4$.

The reaction process of $g-C_{3.6}N_4$

In the three typical stage of the $g-C_{3.6}N_4$ synthetic process, the compound **b** is from the condensation reaction between melamine and glyoxal. Subsequently, the compound **b** is quickly formed from melamine precursor **c** *via* deamination reaction at relatively low temperature. Finally, these heterostructural motifs undergo further polymerization to form the final $g-C_{3.6}N_4$ heterostructure nanosheets **d** at the elevated temperature.



Characterizations

X-ray diffraction (XRD) characterization was carried out on a Bruker AXS D8-Advanced diffractometer with $\text{CuK}\alpha$ radiation ($\lambda = 1.5418 \text{ \AA}$). The composition analyses of the samples were carried on FEI Nova Nano SEM450 with energy dispersive spectroscopy (EDS). Samples for TEM analysis were prepared by depositing a single drop of diluted $\text{g-C}_x\text{N}_4$ dispersion in ethanol on amorphous carbon coated copper grids. TEM images were obtained with a Philips CM 20 operating at 120 kV. High-resolution TEM (HRTEM) and the high-angle annular dark field (HAADF) images were obtained on a Fei Tecnai Osiris with an accelerating voltage of 200 kV. X-ray photoelectron spectroscopy (XPS) measurement was performed on an ESCALAB-MKII spectrometer (Thermo Fisher Scientific) with $\text{Al } K_\alpha$ X-ray radiation as the X-ray source for excitation. Diffuse reflectance spectra (DRS) were measured using a Cary 5000 spectrophotometer fitted with an integrating sphere attachment from 220-850 nm with BaSO_4 as the reference. Infrared spectra were recorded on a Bruker Tensor 27 FTIR spectrometer. Elemental analysis was performed on a FLASH EA 1112 Series NCHS-O analyser. Detailed analyses for O_2 and H_2 were performed on GC-6890 with thermal conductivity detector (TCD) and flame ionization detector (FID)-Methanator (detection limit for CO: $\sim 2 \text{ ppm}$). The soft X-ray absorption spectroscopy (sXAS) experiments were performed at beamline 02B02 at the Shanghai Synchrotron Radiation Facility (SSRF). The bending magnet beamline provides photons with an energy range from 50 to 2000 eV. The photon flux is about $10^{11} \text{ photons s}^{-1}$ and the average energy resolving power is 5000. The beam size at the sample was set to $150\mu\text{m} \times 100\mu\text{m}$. The K-edge of C and N spectra were collected using surface-sensitive total electron yield (TEY) at room temperature in an ultrahigh vacuum chamber with a base pressure better than $1 \times 10^{-9} \text{ Torr}$. The 40 mg $\text{g-C}_3\text{N}_4$ and $\text{g-C}_{3.6}\text{N}_4$ were dispersing into 2 mL of chlorobenzene, and the solution was ultrasounded for 0.5 h. The cleaned glass substrate was placed into the spin coater, and the quantitative solution was dripped onto the entire substrate, and then set as the rotational speed of 3000 rpm for 30 s. After the coating process, the substrate was

taken out and dried in the glove box for 20 min at room temperature, and the the film sample for transient absorption could be obtained. Under ambient conditions, the fs-TA measurements were performed on a Helios pump-probe system (Ultrafast Systems LLC) combined with an amplified femtosecond laser system (Coherent). Optical parametric amplifier (TOPAS-800-fs) provided a 365 nm pump pulse (~ 8 nJ/pulse at the sample), which was excited by a Ti: sapphire regenerative amplifier (Legend Elite-1K-HE; 800 nm), 35 fs, 7 mJ/pulse, 1 kHz) and seeded with a mode-locked Ti: sapphire laser system (Micra 5) and an Nd: YLF laser (Evoluflon 30) pumped. Focusing the 800 nm beams (split from the regenerative amplifier with a tiny portion, ~ 400 nJ/pulse) onto a sapphire plate produced the white-light continuum (WLC) probe pulses (420-780 nm and 820-1600 nm). The pulse-to-pulse fluctuation of the WLC is corrected by a reference beam split from WLC. A motorized optical delay line was used to change the time delays (0-8 ns) between the pump and probe pulses. The instrument response function (IRF) was determined to be ~ 100 fs by a routine cross-correlation procedure. The instrument response function (IRF) was determined to be ~ 100 fs by a routine cross-correlation procedure. A mechanical chopper operated at a frequency of 500 Hz used to modulate the pump pulses such that the fs-TA spectra with and without the pump pulses can be recorded alternately. The temporal and spectral profiles (chirp-corrected) of the pump-induced differential transmission of the WLC probe light (i.e., absorbance change) were visualized by an optical fiber-coupled multichannel spectrometer (with a CMOS sensor) and further processed by the Surface Xplorer software. The sample is measured by pump and probe polarizations oriented at the magic angle. According to the signal amplitude of femtosecond visible and near-infrared TA measurements, at least 5 scans were acquired and averaged to obtain a real data and the high signal-to-noise ratio (SNR) necessary for global analysis.

DFT Calculation Summary

The geometry structures and electronic properties of g - C_3N_4 and g - $C_{3.6}N_4$ were investigated by the Vienna Ab-initio Simulation Package (VASP). The interaction

between valence electrons and the ionic core was simulated by the PAW pseudo-potential of C ($2s^2 2p^2$) and N ($2s^2 2p^3$) potentials. The Perdew-Burke-Ernzerhof (PBE) of the generalized gradient approximation (GGA) was used as the exchange-correlation function in all density functional theory (DFT) calculations. Firstly, the optimized geometry structures of $g\text{-C}_3\text{N}_4$ and $g\text{-C}_{3.6}\text{N}_4$ were obtained from the structural relaxation calculations with the energy cutoff of 400 eV and the energy convergence of 1.0×10^{-4} eV at Gamma point. In the $g\text{-C}_3\text{N}_4$ structure, the triangular melem rings (C_6N_{10} groups) are connected to each other via the N atoms. However, in the $g\text{-C}_{3.6}\text{N}_4$ structure, the $\text{N}=\text{CH}-\text{CH}=\text{N}$ structure (sLink) acts as the bridge between two neighboring C_6N_{10} groups. After geometry optimization, the Monkhorst-Pack k-point meshes of $2 \times 2 \times 1$, the energy cutoff of 400 eV, the energy convergence of 1.0×10^{-4} eV and the hybrid functional of HSE06 were adopted to perform the density of state (DOS) and the projected density of state (PDOS) calculations.

AQY calculation methods

We cited the reference^[2] using the one-step excitation process, producing one H atom from H^+ needs one electron (e.g., one H_2 molecule needs two electrons). Then the AQY could be calculated according to the following Equation:

$$\begin{aligned} \text{AQY}(\%) &= \frac{\text{Number of reacted electrons}}{\text{Number of incident photons}} \times 100\% \\ &= \frac{\text{Number of evolved H}_2 \text{ molecules} \times 2}{\text{Number of incident photons}} \times 100\% \end{aligned}$$

Take $\text{AQY}@400 \text{ nm}$ of $g\text{-C}_{3.6}\text{N}_4$ as an example, $n = 9.62 \times 10^{-6}$, $N_A = 6.02 \times 10^{23}$

$$N = \frac{\mathbf{P} \times \lambda \times \mathbf{t}}{\mathbf{h} \times \mathbf{c}} = 2.317 \times 10^{20}$$

$$\begin{aligned} \text{AQY}(\%) &= \frac{\text{Number of reacted electrons}}{\text{Number of incident photons}} \times 100\% \\ &= \frac{\text{Number of evolved H}_2 \text{ molecules} \times 2}{\text{Number of incident photons}} \times 100\% \end{aligned}$$

$$\begin{aligned}
 &= \frac{N_A \times n \times 2}{N} \times 100\% \\
 &= \frac{N_A \times n \times 2}{N} \times 100\% \\
 &= 4.99\%
 \end{aligned}$$

Water Splitting Measurements

Photocatalytic overall water splitting reactions were carried out in a system containing a photoreactor (Pyrex glass) and a closed gas circulation system (LabSolar-H2, Beijing Trusttech Co. Ltd., China) operated at room temperature with 100 mL of preboiled deionized water to split. A 300 W xenon lamp (PLS-SXE 300, Beijing Trusttech Co. Ltd., China) was adopted as the light source. The light intensity for the water splitting was controlled at $\sim 100 \text{ mW cm}^{-2}$. 100 mg of the photocatalysts $\text{g-C}_3.6\text{N}_4$ were dispersed in 100 mL DI-water without co-catalyst, additive and sacrificial electron donor. The reactant solution was evacuated several times to remove air thoroughly and irradiated a 300 W Xe lamp with a long-pass cutoff filter allowing $\lambda > 400 \text{ nm}$ (PLS-SXE 300, Beijing perfectlight Co. Ltd, China). The generated hydrogen and oxygen were measured by a gas chromatograph (GC7890-2, Techomp) operating at isothermal conditions with semicapillary columns (molecular sieves 5 Å) and Ar as the carrier gas. The five cycles with time interval of 24 hours were performed.

2. Supplementary Figures and Tables

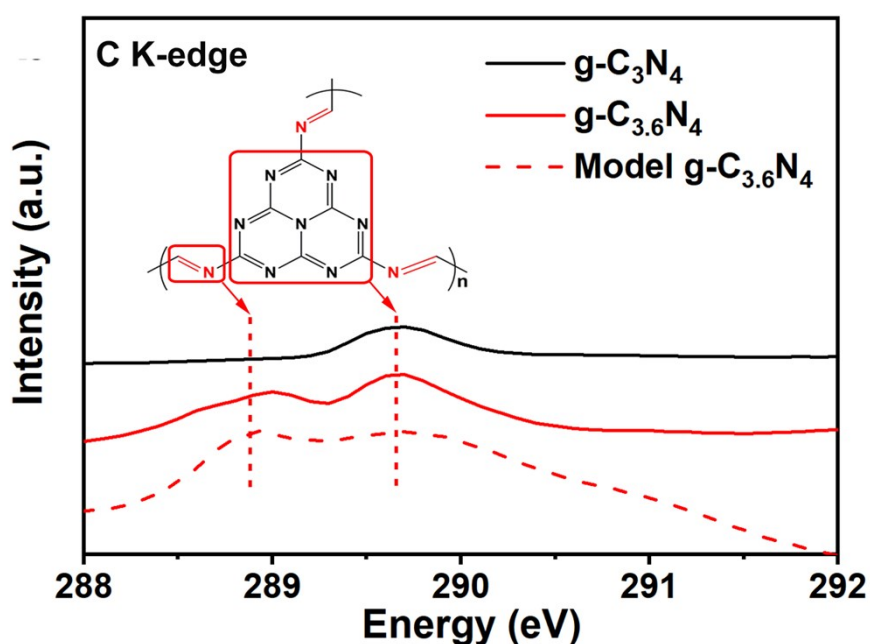


Figure S1. C K-edge XANES experimental spectra of g-C₃N₄ (black curve) and g-C_{3.6}N₄ (red curve), and theoretical spectra of g-C_{3.6}N₄ (red dashed curve).

Table S1. Elemental analysis of pristine g-C₃N₄ and g-C_xN₄ using XPS.

Molar ratio of glyoxal and melamine	As-synthesized g-C _x N ₄
Pure melamine	g-C _{3.02} N ₄
3:8	g-C _{3.22} N ₄
3:4	g-C _{3.63} N ₄
9:8	g-C _{3.81} N ₄

Table S2. Elemental analysis of pristine g-C₃N₄ and g-C_xN₄ using elemental analysis analyser.

Molar ratio of glyoxal and melamine	As-synthesized g-C _x N ₄
Pure melamine	g-C _{3.03} N ₄
3:8	g-C _{3.21} N ₄
3:4	g-C _{3.64} N ₄
9:8	g-C _{3.83} N ₄

Table S3. C-C and C=N percentages in g-C_xN₄ obtained using XPS.

Entry	g-C _{3.2} N ₄	g-C _{3.6} N ₄	g-C _{3.8} N ₄
C-C group	8.3 %	11.5 %	19.6 %
C=N group	14.1 %	17.1 %	20.9 %

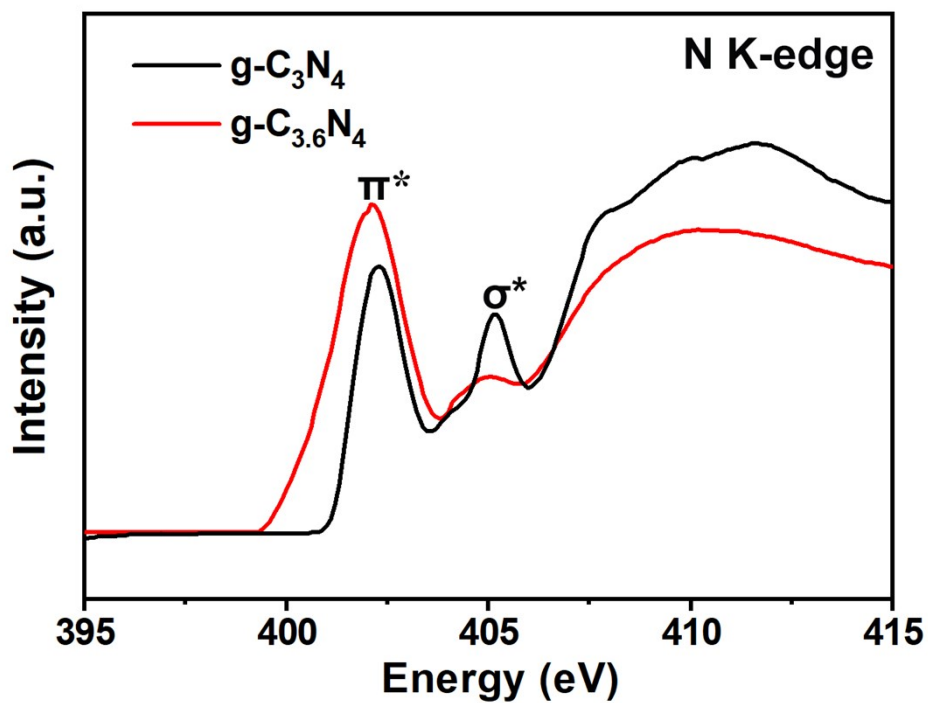


Figure S2. N K-edge XANES spectra of g-C₃N₄ and g-C_{3.6}N₄.

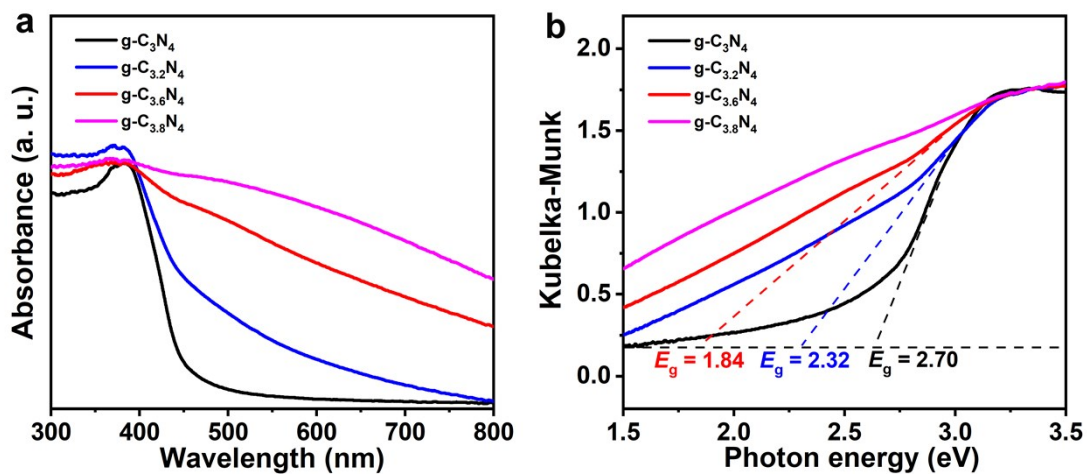


Figure S3. (a) UV-vis absorption spectra and (b) transformed Kubelka-Munk function plots of $g\text{-C}_3\text{N}_4$, $g\text{-C}_{3.2}\text{N}_4$, $g\text{-C}_{3.6}\text{N}_4$, and $g\text{-C}_{3.8}\text{N}_4$. In (b), the horizontal black dash line marks the baseline; the other dash lines are the tangents to the curves.

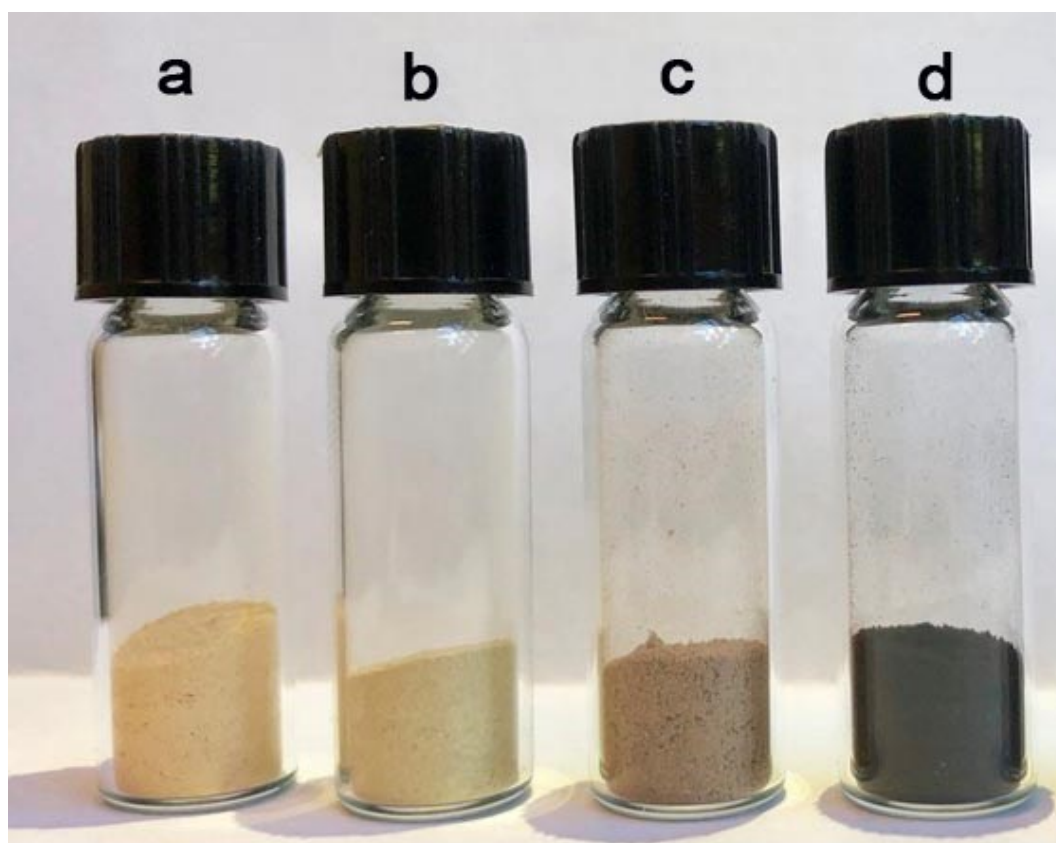


Figure S4. $g\text{-C}_x\text{N}_4$ sample photographs: (a) $g\text{-C}_3\text{N}_4$, (b) $g\text{-C}_{3.2}\text{N}_4$, (c) $g\text{-C}_{3.6}\text{N}_4$, and (d) $g\text{-C}_{3.8}\text{N}_4$.

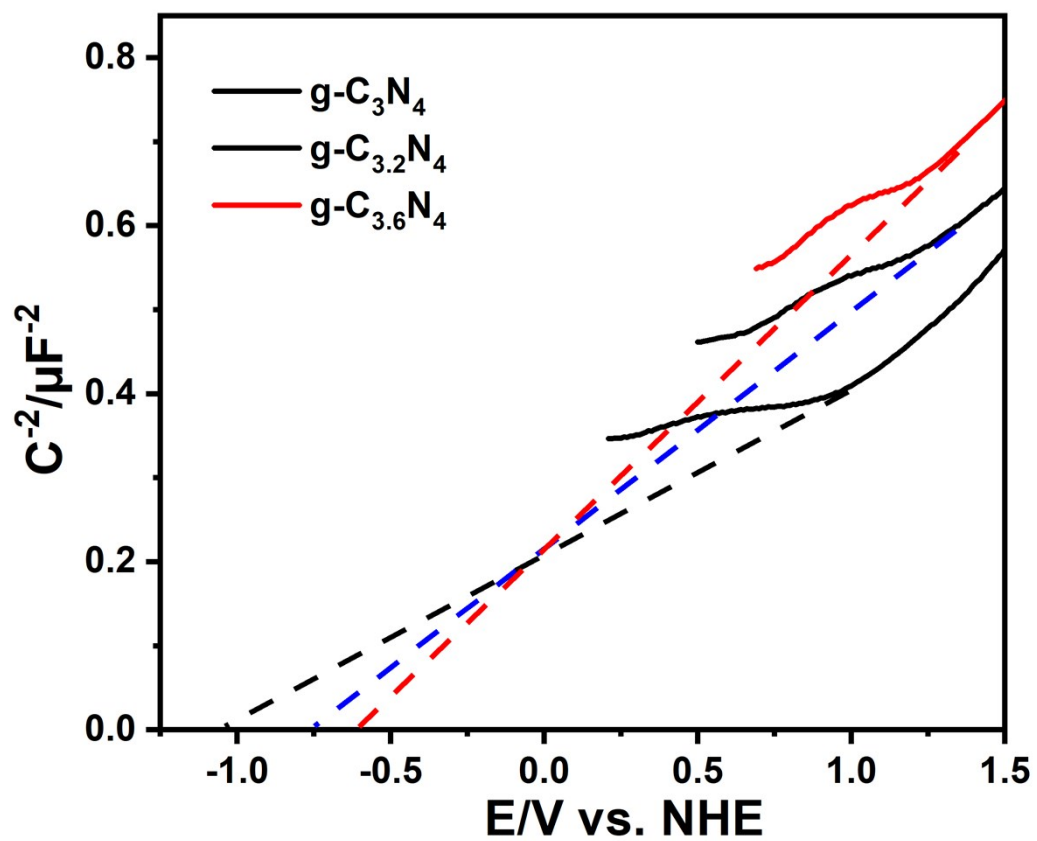


Figure S5. Mott-Schottky plots of $\text{g-C}_3\text{N}_4$, $\text{g-C}_{3.2}\text{N}_4$, and $\text{g-C}_{3.6}\text{N}_4$ electrodes in 0.2 M Na_2SO_4 ($\text{pH}=7$).

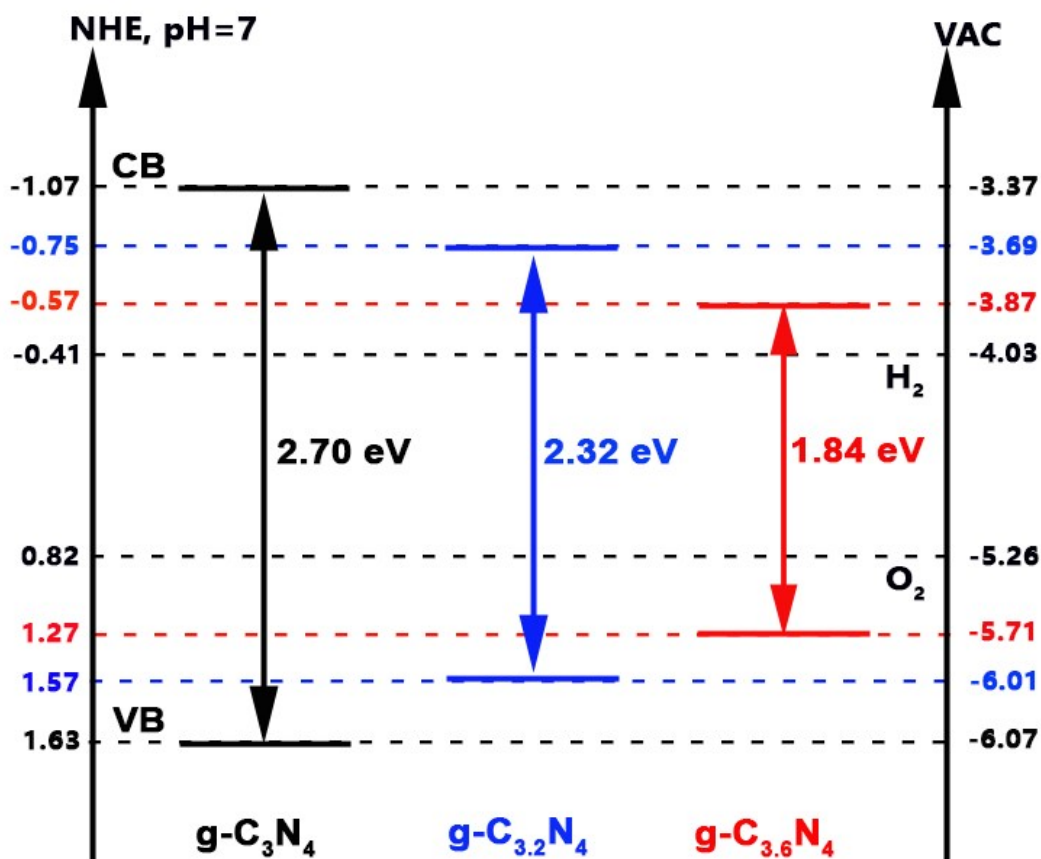


Figure S6. Band levels of $g\text{-C}_x\text{N}_4$ calculated by optical absorption and typical electrochemical Mott-Schottky method (VB = valence band; CB = conduction band).

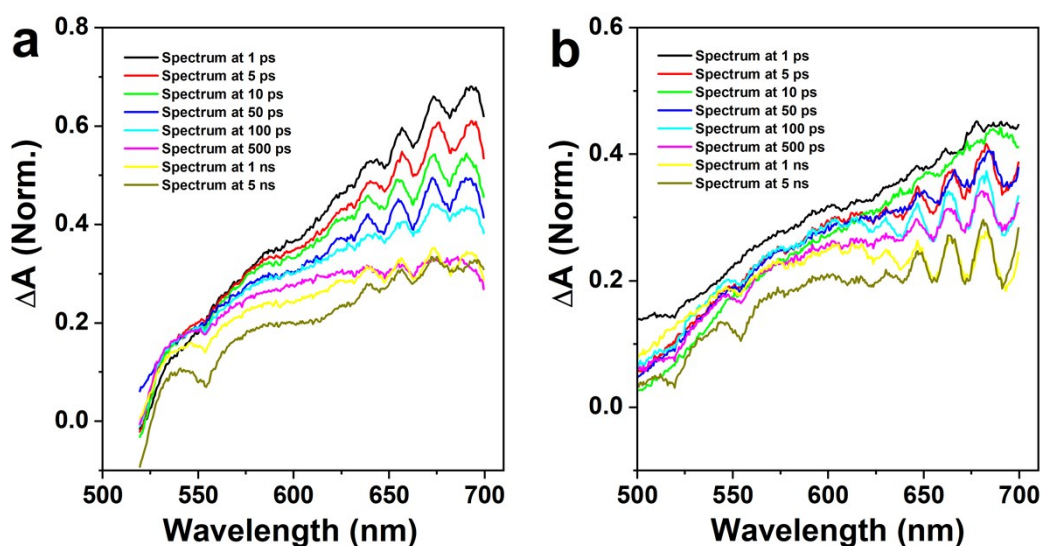


Figure S7. Normalized TAS spectra of: (a) $g\text{-C}_3\text{N}_4$ and (b) $g\text{-C}_{3.6}\text{N}_4$ at short time delay at 630 nm.

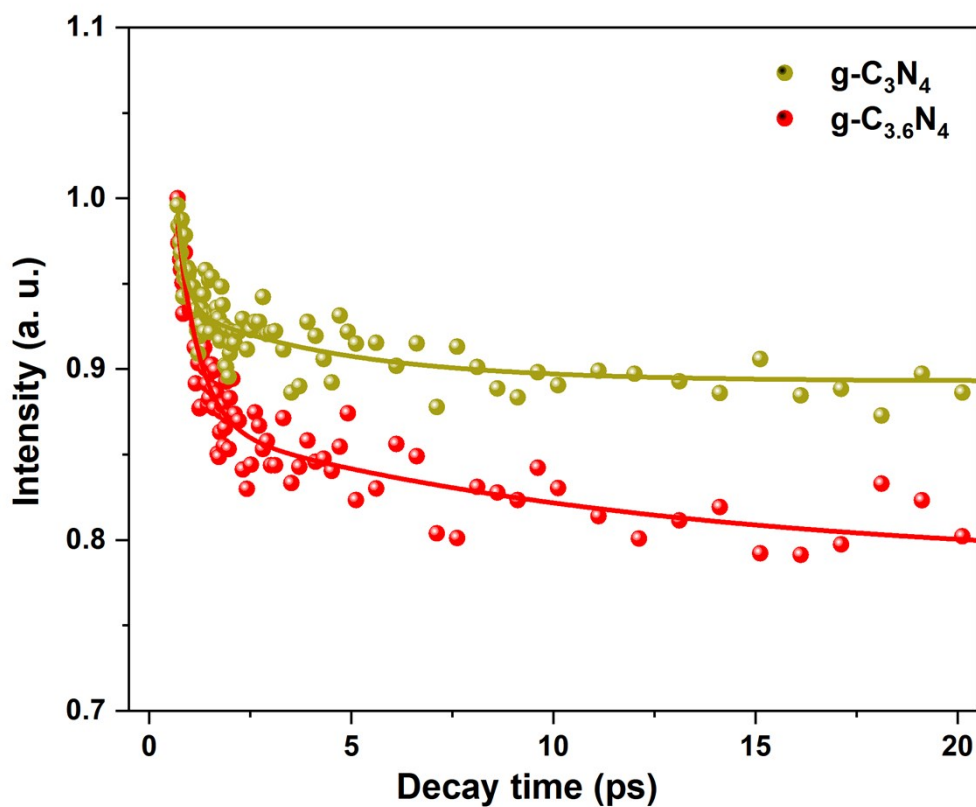


Figure S8. The decay curves of g-C₃N₄ and g-C_{3.6}N₄ at 630 nm.

Table S4. Summary of different time constants (in the 0 to 20 ps range) at 700 nm fitted using a two exponential decay function: $y = y_0 + A_1 e^{\frac{-x}{\tau_1}} + A_2 e^{\frac{-x}{\tau_2}}$

System	τ_1	τ_2
g-C ₃ N ₄	0.22 ± 0.07 (96%)	4.01 ± 1.59 (4%)
g-C _{3.6} N ₄	0.55 ± 0.10 (83%)	11.58 ± 7.10 (17%)

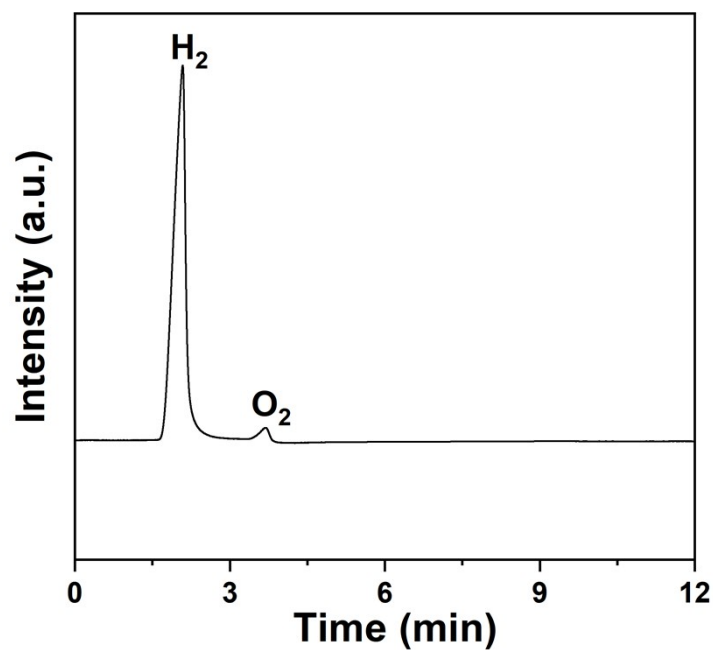


Figure S9. The GC data of g-C_{3.6}N₄ catalyzing water splitting to H₂ and O₂ under visible light irradiation (by a 300 W Xe lamp using a long-pass cutoff filter allowing $\lambda > 420$ nm).

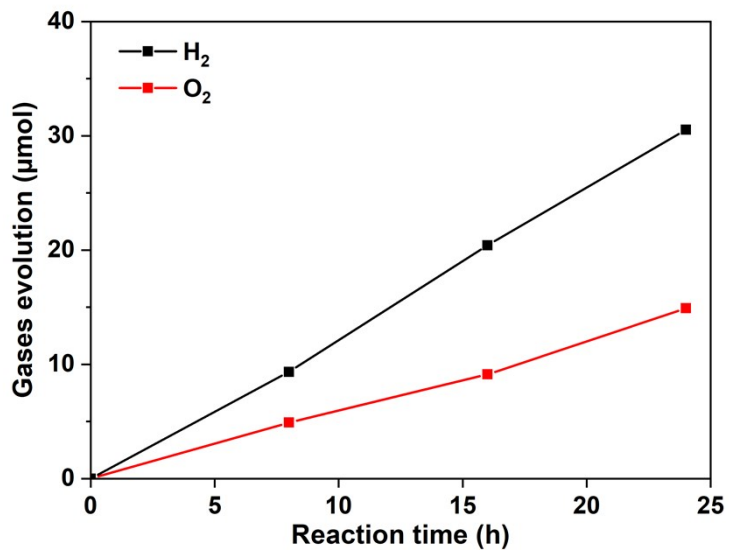


Figure S10. g-C_{3.2}N₄ catalyzed water splitting to H₂ and O₂ under visible light irradiation (by a 300 W Xe lamp using a long-pass cutoff filter allowing $\lambda > 420$ nm).

Table S5 Summary of the overall water splitting performance of g-C₃N₄ based catalysts without co-catalyst.

Catalyst	Water source	Light source	Incident light	H ₂ rate	O ₂ rate	Ref.
		Xe Lamp		($\mu\text{mol/h}\cdot\text{g}$)	($\mu\text{mol/h}\cdot\text{g}$)	
g-C _{3,6} N ₄	Pure water	300 W	> 420 nm	75.3	36.6	This work
NGO-QDs	Pure water	300 W	> 420 nm	6.0	3.0	[3]
C-dot/C ₃ N ₄	Pure water	300 W	> 420 nm	104.0	51.3	[4]

3. Supplementary References

- [1] Liu H., Li X. X., Liu, X. Y., Ma, Z. H., Yin Z. Y., Yang W. W., Yu Y. S. *Rare Met.*, **2021**, 40, 808-816.
- [2] Zhao, D., Wang, Y., Dong, C. L., Huang, Y. C., Chen, J., Xue, F., Guo, L. *Nature Energy*, **2021**, 1-10.
- [3] Yeh, T. F.; Teng, C. Y.; Chen, S. J.; Teng H. *Adv. Mater.* **2014**, 26, 3297.
- [4] Liu, J.; Liu, Y.; Liu, N. Y.; Han, Y. Z.; Zhang, X.; Huang, H.; Lifshitz, Y.; Lee, S. T.; Zhong, J.; Kang, Z. H. *Science* **2015**, 347, 970.